



$^{240+239}\text{Pu}$ DEPOSITIONAL SIGNATURES AS A VIABLE GEOCHRONOLOGICAL TOOL IN THE AMAZON BASIN

LUCIANA M SANDERS¹, KATHRYN H TAFFS¹, DEBRA STOKES¹,
ALEX ENRICH-PRAST^{2,3} and CHRISTIAN J SANDERS⁴

¹School of Environment, Science and Engineering, Southern Cross University, P.O. Box 157, Lismore, NSW 2480, Australia

²Department of Environmental Change, Linköping University, Linköping, Sweden

³Departamento de Botânica, Instituto de Biologia, Universidade Federal do Rio de Janeiro, Rio de Janeiro, Brazil

⁴National Marine Science Centre, Southern Cross University, Coffs Harbour, 2450 NSW, Australia

Received 1 January 2017

Accepted 21 April 2017

Abstract: Anthropogenic radionuclide signatures associated with nuclear testing are increasingly utilized in environmental science to explore recent sedimentation. In this study, we assess the suitability of Pu radioisotope analysis in floodplain lake environments in the Amazon Basin to form geochronologies during the 20th century. The $^{240}\text{Pu} + ^{239}\text{Pu}$ ($^{240+239}\text{Pu}$) signatures in six sediment cores indicate sediment accumulation rates in the floodplain lakes of the major rivers; Amazon (2.3 mm year⁻¹), Tapajós (10.2 and 2.4 mm year⁻¹) and Madeira (3.4, 4.2 and 6.2 mm year⁻¹). The results from this study show that $^{240+239}\text{Pu}$ fallout activities, and the well documented ($^{240}\text{Pu}/^{239}\text{Pu}$) atomic ratios of the above ground nuclear tests which began in the 1950's, are sufficient and well preserved in Amazon floodplain lake sediments to infer chronologies. Lead-210 dating analyses in the same sediment cores produced comparable sediment accumulation rates at three of the six sites. The differences between dating methods may be attributed to the different time scale these dating methods represent and/or in the solubility between Pb and Pu along the sediment column. The geochronologies derived from the $^{240+239}\text{Pu}$ and ^{210}Pb dating methods outlined in this work are of interest to identify the effects of changing sediment accumulation rates during the previous century as a result of development, including deforestation, along the Amazon Basin which increased towards the middle of the 20th century. This study shows that Pu dating provides a viable alternative geochronology tool for recent sediment accumulation (previous ~60 years) along the Amazon Basin.

Keywords: plutonium dating, geochronology, Amazon floodplain lakes, sedimentation.

1. INTRODUCTION

Anthropogenic radionuclides from the Cold War era above-ground nuclear tests are routinely used to date sediments around the globe (Ketterer *et al.*, 2004a; Sanders *et al.*, 2016; Sanders *et al.*, 2010). These radio-

nuclides, including Pu isotopes, fission products (^{137}Cs , ^{90}Sr , ^{129}I) and activation products (^3H , ^{14}C), were deposited globally from the early 1950's to the late 1960's from USA and former Soviet Union nuclear bomb testing (Abril, 2003; Alhajji *et al.*, 2014). Plutonium is very useful as a chronological tool as the ^{239}Pu and ^{240}Pu atomic ratios ($^{240}\text{Pu}/^{239}\text{Pu}$) can be used to indicate the source. For instance, $^{240}\text{Pu}/^{239}\text{Pu}$ atomic ratios from global fallout (~0.18) differ from well-known $^{240}\text{Pu}/^{239}\text{Pu}$ atomic ratios from events such as Fukushima (0.30–0.33) (Zheng *et al.*, 2012) and Chernobyl (~0.43) (Ketterer *et al.*, 2004b). These distinct ratios may be useful for separating phases

Corresponding author: L. M. Sanders
e-mail: l.sanders.13@student.scu.edu.au

of sediment deposition because the nuclear accidents and testing dates are well known (Kelley *et al.*, 1999).

There are six principal radio-isotopes of Plutonium; ^{238}Pu ($t_{1/2} = 87.74$ years), ^{239}Pu ($t_{1/2} = 241,100$ years), ^{240}Pu ($t_{1/2} = 6,561$ years), ^{241}Pu ($t_{1/2} = 14.29$ years), ^{242}Pu ($t_{1/2} = 373,000$ years) and ^{244}Pu ($t_{1/2} = 8.3 \times 10^7$ years). The isotopes ^{238}Pu , ^{239}Pu , ^{240}Pu , ^{242}Pu and ^{244}Pu decay through α emission, whereas ^{241}Pu decays through β emissions, producing ^{241}Am ($t_{1/2} = 432.6$ years). Sediments where $^{240}\text{Pu} + ^{239}\text{Pu}$ ($^{240+239}\text{Pu}$) activity is first detected represents pre nuclear bomb deposited sediments and hence pre early 1950s deposition. Because plutonium is relatively immobile under both freshwater and saltwater conditions (Ketterer *et al.*, 2004b; Zheng and Yamada, 2004) it is an ideal chronology tool in lake environments.

Anthropogenic radionuclides from atmospheric fallout have been widely used as a tracer of sedimentation processes in the Northern Hemisphere (Abril, 2003; Alhajji *et al.*, 2014; Ketterer *et al.*, 2004a; Omokheyeke *et al.*, 2014; Pourcelot *et al.*, 2003; Quinto *et al.*, 2013; Todorović *et al.*, 2013; Wu *et al.*, 2011; Zheng and Yamada, 2004), and $^{240+239}\text{Pu}$ atomic ratios have been used with great success in fresh water lake studies (Cao *et al.*, 2017; Ketterer *et al.*, 2004a; Łokas *et al.*, 2017; Mietelski *et al.*, 2016a; Wu *et al.*, 2011). Furthermore, plutonium radioisotopes ($^{239+240}\text{Pu}$) have been successfully used as a chronostratigraphic marker in Australia and New Zealand (Everett *et al.*, 2008; Leslie and Hancock, 2008; Sanders *et al.*, 2016; Tims *et al.*, 2013). However, Pu radionuclides have not been used extensively in the South American continent.

The timeframe of when anthropogenic plutonium was deposited globally closely matches periods of rapid and extensive land use change in the Amazon Basin (Barlow *et al.*, 2016). As such, Pu isotopes may be a valuable tool in assessing sedimentation changes in the Amazon floodplains associated with deforestation and/or urbanization. The aim of this study is to assess the potential of $^{240+239}\text{Pu}$ signatures as a geochronology tool to determine the sediment accumulation rates in the Amazon floodplain lakes of the major rivers in the Amazon forest. To achieve this aim, six sediment cores were collected from differing floodplain lakes to construct sediment dates from 1950 to present using anthropogenic ($^{239+240}\text{Pu}$) radionuclide signatures. These deposition chronologies were then compared to ~100 year records using natural (^{210}Pb , ^{226}Ra) radionuclide tracers. The dating methods outlined in this work will be used to form geochronologies during the 20th century, a timeframe that the Amazon has experienced substantial deforestation and significant changes in sediment loads (Barlow *et al.*, 2016; Rowland *et al.*, 2015).

2. MATERIAL AND METHODS

Six sediment cores were collected from Amazon floodplain lakes adjacent to the Amazon and Tapajos Rivers (PA2 and PA9 adjacent the Tapajos River, and PA10 adjacent the Amazon River), and another three PP, RM and PZC, adjacent to the Madeira River near the city of Porto Velho, Brazil (Fig. 1). The sediment cores were collected using percussion and rotation to minimize sediment compression. The sediment cores ranged from 25 to 70 cm length. The sediment cores were sub sampled in 2 cm intervals. Dry bulk density (DBD, g cm^{-3}) was determined as the dry sediment weight (g) divided by the initial volume (cm^3).

The laboratory preparation for Pu analysis followed the method of Ketterer *et al.* (2004a, 2004b) having been scaled to accommodate larger sample masses. Sample aliquots ranging from 10 to 29 grams were dry-washed at 600°C for 16 hours, and leached with 50 mL of 16 M HNO_3 . The leaching was conducted overnight at 80°C with added ^{242}Pu yield tracer (NIST 4334g, 19 picograms). Acid leaching (as opposed to complete dissolution with HF) is known to solubilize stratospheric fallout Pu, and there is little possibility that refractory HNO_3 -insoluble Pu exists, at least in the Brazilian coastal plain setting (Sanders *et al.*, 2010).

The leachates were diluted to 100 mL, filtered to remove solids, and the aqueous solutions were processed with TEVA resin (Eichrom, Lisle, IL, USA) in order to chemically isolate 3.0 mL Pu fractions in aqueous ammonium oxalate solution suitable for measurements by sector ICPMS. Pu determinations were performed using a VG Axiom MC operating in the single collector (electron multiplier) mode. The system was used with an APEX HF system (ESI Scientific, Omaha, NE, USA) with an uptake rate of 0.4 mL/minute. Qualitative mass spectral scans (averages of 50 sweeps over the mass range 237.4–242.6) were collected for selected samples prior to the electrostatic sector quantitative scanning of $^{238}\text{U}^+$, $^{239}\text{Pu}^+$, $^{240}\text{Pu}^+$, and $^{242}\text{Pu}^+$. Detection limits were evaluated based upon the analysis of two blanks. A detection limit of 0.01 Bq/kg of $^{240+239}\text{Pu}$ is applicable for samples of nominal 25 gram mass (Ketterer *et al.*, 2004a; Ketterer *et al.*, 2004b; Ketterer and Szechenyi, 2008).

For ^{210}Pb dating the sediment cores were analyzed for radionuclide concentrations in an HPGe gamma well detector (Appleby and Oldfield, 1992). Freeze dried and ground sediments were packed and sealed in gamma tubes. The ^{210}Pb and ^{226}Ra activities were calculated by using a factor that includes the gamma detector efficiency, as previously determined from certified reference material IAEA-300 (Baltic Sea Sediment) and the gamma-ray intensity. The ^{210}Pb and ^{226}Ra activities were

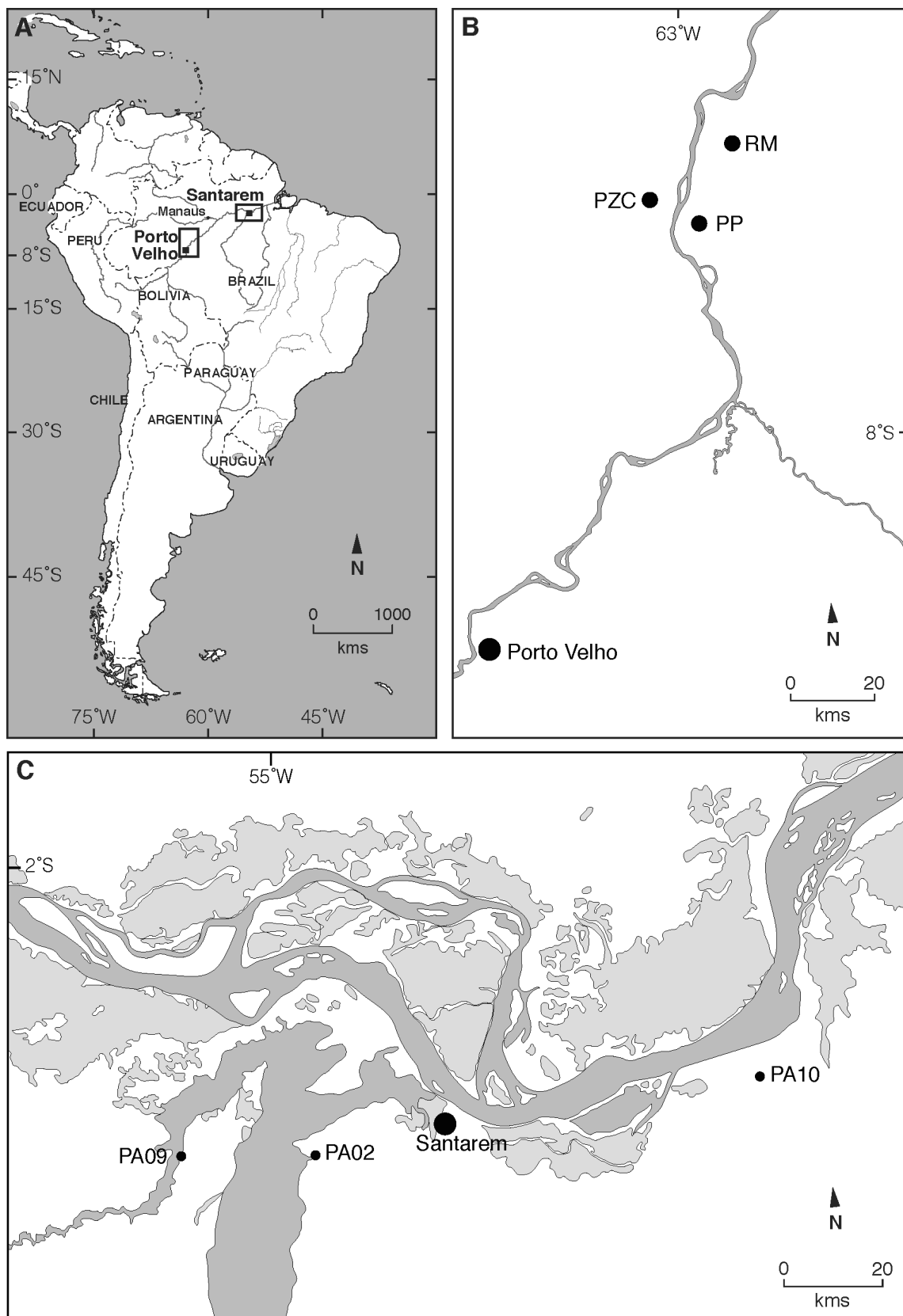


Fig. 1. Study area: A) South America; B) Porto Velho region showing study sites RM, PP, PZC floodplain lakes adjacent to the Madeira River and; C) Santarem region showing study sites PA2 and PA9 floodplain lakes located near the Tapajós River, PA10 sediment core from a floodplain lake directly influenced by the Amazon River.

measured using the 46.5 KeV and 351.9 KeV gamma peaks, respectively (Sanders *et al.*, 2016). Prior to radionuclide measurements, samples were set aside for at least 3 weeks, to allow for ^{222}Rn ingrowth and to establish secular equilibrium between ^{226}Ra and its granddaughter ^{214}Pb . The excess ^{210}Pb activities (referred to as $^{210}\text{Pb}_{\text{ex}}$ from here onward) were determined by subtracting the ^{226}Ra concentrations (*i.e.* supported ^{210}Pb) from the total ^{210}Pb concentrations. The sediment accumulation rates (cm yr^{-1}), taken from the ^{210}Pb constant initial concentration (CIC) dating method, and the dry bulk density (g cm^{-3}) in each interval (cm) were used to determine mass accumulation rates (Appleby and Oldfield, 1992).

3. RESULTS

The dry bulk densities (g cm^{-3}) are shown in **Table 1**. The Pu atomic ratios in the six sediment cores indicate that the Pu is originating from stratospheric fallout (plutonium isotopic ratios $^{240}\text{Pu}/^{239}\text{Pu}$) which ranged from 0.17 to 0.19 in the sediment cores near the Tapajos and Amazon Rivers and 0.16 to 0.20 in the sediment cores near the Madeira River (**Table 2**). There is no consistent activity pattern down the sediment profiles that resembles

the expected atmospheric deposition history. Therefore, it is not possible to assess a 1963 peak deposition date from this profile. However the material below the depth where $^{240+239}\text{Pu}$ first appears was deposited pre-bomb (that is, prior to the early 1950s) (Sanders *et al.*, 2014b; Sanders *et al.*, 2010). From the three sediment cores collected in proximity to the Tapajos and Amazon Rivers (PA2, PA9 and PA10), plutonium was first detected at the 14–16 cm interval for PA2, with the highest concentrations at the 10–12 cm interval of 0.533 ± 0.037 . In PA9 plutonium was first detected at the 58–62 cm interval with the highest concentrations at the 42–46 cm interval of 0.0925 ± 0.022 Bq/kg $^{240+239}\text{Pu}$ (**Fig. 2**). In core PA10, plutonium is first detected in the 14–16 cm interval, and has a maximum concentration of 0.717 ± 0.005 Bq/kg $^{240+239}\text{Pu}$ at the 16–18 cm interval. In the three sediment cores near the Madeira River (PP, PZC and RM), plutonium is first detected at the 20–22 cm interval for PP with the highest concentration of 0.129 ± 0.010 Bq/kg $^{240+239}\text{Pu}$ at 12–14 cm interval. In PZC plutonium was first detected at 26–28 cm interval with the highest concentration at the 12–14 cm interval of 0.127 ± 0.011 Bq/kg $^{239+240}\text{Pu}$. In core RM plutonium is first detected in the 38–40 cm interval and has a maxi-

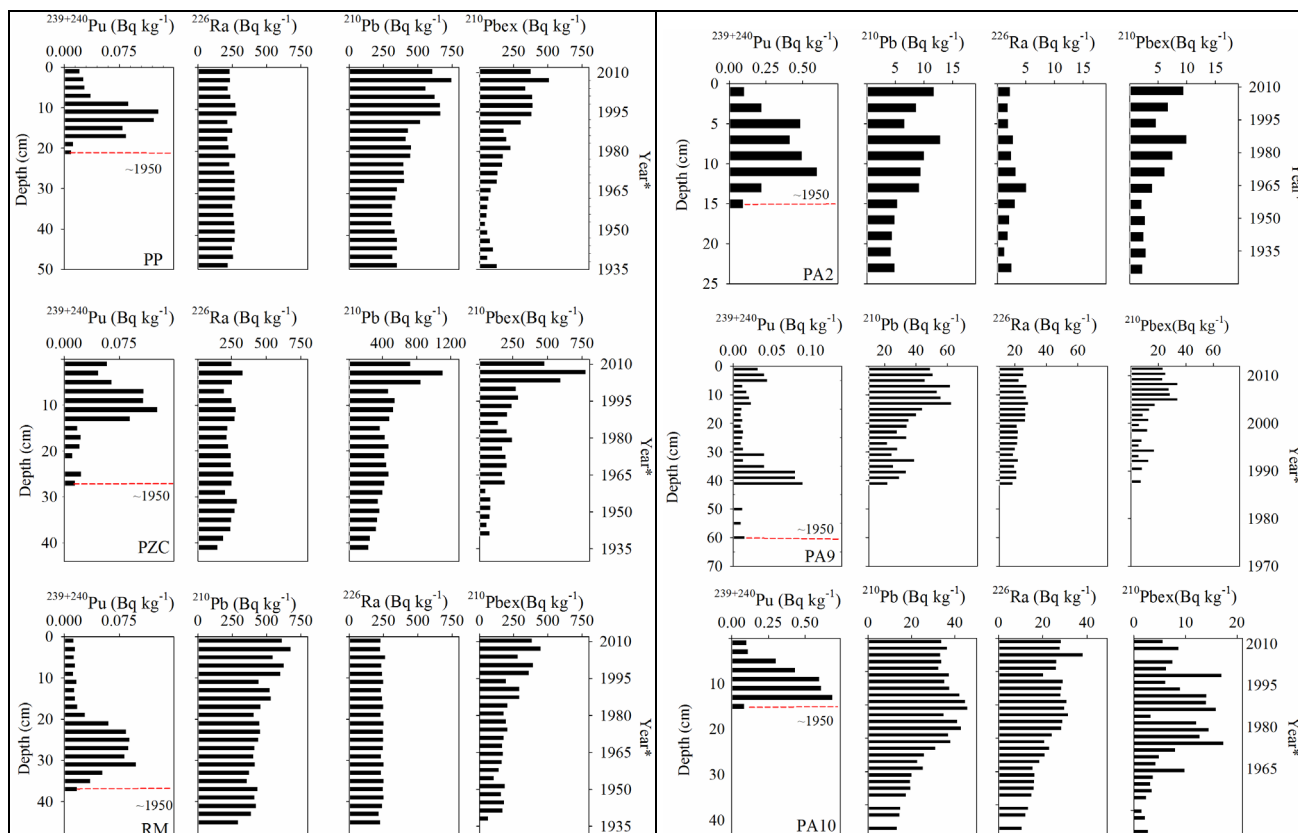


Fig. 2. $^{239+240}\text{Pu}$, ^{210}Pb , ^{226}Ra and $^{210}\text{Pb}_{\text{ex}}$ profiles from the six sediment cores in this work. The first occurrence of $^{239+240}\text{Pu}$ indicates ~ 1950 when these radionuclides were first introduced into the atmosphere. The ~ 1950 mark on the $^{210}\text{Pb}_{\text{ex}}$ profiles are based on the sediment accumulation rates dated through the Constant Initial Concentration (CIC) approach (Appleby and Oldfield, 1992). PP, PZC, RM, PA2, PA9, PA10 – study sites.

Table 1. Depth profiles of dry bulk density (DBD) ($g\ cm^{-3}$) and mass accumulation rates (MAR) ($g\ cm^{-2}\ year^{-1}$) of the six sediment cores (PA2, PA9, PA10, RM, PP, PZC) studied in this work.

Depth (cm)	PA2		PA9		PA10		RM		PP		PZC	
	DBD	MAR										
0–2	0.54	0.18	0.48	0.53	1.01	0.34	0.65	0.37	0.89	0.28	0.74	0.33
2–4	0.55	0.19	0.53	0.58	0.89	0.30	0.63	0.36	0.81	0.26	0.56	0.25
4–6	0.58	0.20	0.60	0.66	1.03	0.35	0.77	0.44	0.83	0.26	0.62	0.28
6–8	0.59	0.20	0.56	0.61	1.07	0.36	0.69	0.39	0.84	0.27	0.72	0.32
8–10	0.62	0.21	0.58	0.63	1.04	0.35	0.71	0.40	0.77	0.25	0.72	0.32
10–12	0.61	0.21	0.59	0.65	1.05	0.36	0.75	0.43	0.78	0.25	0.76	0.34
12–14	0.57	0.19	0.63	0.70	1.14	0.39	0.70	0.40	0.94	0.30	0.72	0.32
14–16	0.62	0.21	0.66	0.72	1.10	0.37	0.68	0.39	1.02	0.33	0.91	0.41
16–18	0.58	0.20	0.63	0.69	0.99	0.34	0.66	0.37	1.05	0.33	0.71	0.32
18–20	0.57	0.19	0.62	0.68	1.07	0.36	0.64	0.36	1.00	0.32	0.77	0.34
20–22	0.59	0.20	0.63	0.70	0.96	0.33	0.74	0.42	0.90	0.29	0.78	0.35
22–24	0.59	0.20	0.62	0.68	1.00	0.34	0.70	0.40	1.06	0.34	0.72	0.32
24–26	0.58	0.20	0.61	0.68	0.97	0.33	0.67	0.38	1.00	0.32	0.81	0.37
26–28	0.58	0.20	0.66	0.73	1.05	0.36	0.77	0.44	0.94	0.30	0.96	0.43
28–30	0.59	0.20	0.72	0.79	0.95	0.32	0.71	0.40	0.96	0.31	0.81	0.37
30–32	0.62	0.21	0.71	0.78	0.95	0.32	0.81	0.46	0.96	0.31	0.78	0.35
32–34	0.55	0.19	0.68	0.75	1.30	0.44	0.81	0.46	1.09	0.35	0.81	0.37
34–36	0.57	0.19	0.63	0.69	1.57	0.53	0.77	0.44	1.05	0.34	0.92	0.41
36–38	0.56	0.19	0.70	0.77	1.36	0.46	0.74	0.42	1.00	0.32	0.72	0.33
38–40	0.53	0.18	0.69	0.76	1.36	0.46	0.70	0.40	0.99	0.32	0.77	0.35
40–42	0.54	0.18	0.70	0.77	1.45	0.49	0.72	0.41	0.98	0.31	0.82	0.37
42–44	0.55	0.19	0.69	0.76	1.55	0.53	0.72	0.41	0.98	0.31	0.90	0.40
44–46	0.69	0.23	0.70	0.77	1.75	0.60	0.84	0.48	1.06	0.34	0.95	0.43
46–48	0.68	0.23	0.72	0.79	1.47	0.50	0.77	0.44	0.44	0.32	0.86	0.39
48–50	0.62	0.21	0.68	0.75	1.36	0.30	0.74	0.42	0.42	0.32	0.72	0.39
Average	0.59	0.20	0.64	0.70	1.18	0.39	0.72	0.41	0.91	0.31	0.78	0.35
Stand Dev	0.04	0.01	0.06	0.07	0.23	0.08	0.05	0.03	0.17	0.03	0.09	0.04

imum concentration of $0.098 \pm 0.013\ Bq/kg$ ²⁴⁰⁺²³⁹Pu (Fig. 2). A grand average for ²⁴⁰Pu/²³⁹Pu atomic ratios were 0.187 ± 0.019 , as determined from the collective core intervals and propagating the standard deviations from each sediment core.

Fig. 2 shows the ²¹⁰Pb, ²²⁶Ra and subsequent ²¹⁰Pb_(ex) sediment core profiles. A general downcore decrease in ²¹⁰Pb_(ex) activity was found in five of the six sediment cores (Fig. 2), with only PA10 showing substantial sediment mixing at the surface intervals. For sediment core PA9, ²¹⁰Pb analysis was conducted from the surface down to 40–42 cm depth interval. However for the Pu analyses in this same sediment core, samples were combined in 4 cm intervals from the 42–46 until the 68–72 cm depth intervals. No ²⁴⁰⁺²³⁹Pu was found in the 62–66 and 66–70 cm intervals. Therefore the 1950 date was established to be at the 58–62 cm depth interval representing the onset of nuclear bomb testing, as ²⁴⁰⁺²³⁹Pu was only introduced into the atmosphere after the early 1950s.

The ²⁴⁰⁺²³⁹Pu and ²¹⁰Pb inventories and fluxes shown on Table 2 are based on the entire core. These inventories give an integrated view of the total supply of ²⁴⁰⁺²³⁹Pu and ²¹⁰Pb_{ex} to the water column from multiple sources. The ²⁴⁰⁺²³⁹Pu and ²¹⁰Pb_{ex} input comes from the atmosphere and runoff, which should be included when consid-

ering the sources to the sedimentation inventories. The ²¹⁰Pb_{ex} inventories may also include an *in situ* production source. The mass accumulation rates ($g\ cm^{-2}\ year^{-1}$), noted on Table 2, were determined by multiplying the sedimentation rates ($cm\ year^{-1}$), by the dry bulk densities ($g\ cm^{-3}$) for each sediment core interval.

4. DISCUSSION

The ²⁴⁰⁺²³⁹Pu results are consistent with the ²⁴⁰Pu/²³⁹Pu of 0.180 ± 0.014 discussed by Kelley *et al.* (1999), indicating that the source is from Cold War era above-ground nuclear tests deposited globally from the

Table 2. Sediment accumulation rates ($mm\ year^{-1}$) and inventories ($mBq\ cm^{-2}$) based on the ²¹⁰Pb and ²³⁹⁺²⁴⁰Pu sediment dating methods.

Study Site	²¹⁰ Pb ($mm\ year^{-1}$)	²¹⁰ Pb ($Bq\ cm^{-2}$)	²³⁹⁺²⁴⁰ Pu ($mm\ year^{-1}$)	²³⁹⁺²⁴⁰ Pu ($mBq\ cm^{-2}$)	Major River
PA2	2.7	6.5	2.4	4.9	Tapajos
PA9	18.6	7.0	10.2	1.0	Tapajos
PA10	8.2	53.6	2.3	0.5	Amazon
PP	6.2	22.4	3.4	2.7	Madeiras
PZC	5.8	3.1	4.2	2.0	Madeiras
RM	6.1	40.2	6.2	3.7	Madeiras

early 1950's to the late 1960's (Abril, 2003; Alhajji *et al.*, 2014). Furthermore, these values are in good agreement with the reported $^{240}\text{Pu}/^{239}\text{Pu}$ in southern Equatorial (0–30°S) fallout reported by Kelley *et al.* (1999), who determined an average $^{240}\text{Pu}/^{239}\text{Pu}$ atomic ratio of 0.173 ± 0.027 . The detected plutonium ratio is directly related to anthropogenic introduction to the environment through nuclear bomb testing in the 1950s (Ketterer and Szechenyi, 2008). This affixes an upper limit on the average sedimentation rate of near 2.4 mm year^{-1} in core PA2, $10.2 \text{ mm year}^{-1}$ in sediment core PA9 and 2.3 mm year^{-1} in core PA10 for the lakes near the Porto Velho regions and 3.4 , 4.2 and 6.2 mm year^{-1} for the sediment cores PP, PZC and RM, respectively, near the Santarem region (Fig. 1).

The mass accumulation rate results indicate that even though higher plutonium peak concentrations are observed in the PA10 sediment core, the MAR is greater in the PA9 sediment core (Table 1). The lower $^{240+239}\text{Pu}$ mass accumulation rates in the other sediment cores may be due to dilution from a large sediment load or possibly a result of grain size differences, as the waters vary from fine grain sediment-laden Amazon River to the relatively high concentrations of sand in the Tapajós Rivers (Junk *et al.*, 2015).

There appears to be large sediment focusing, a process whereby water turbulence moves sediment from shallower to deeper zones of a lake (Blais and Kalff, 1995), in the floodplain lakes in this work. This is because the initial atmospheric fallout flux of $^{240+239}\text{Pu}$ is fairly well known and much lower than was found in this study (Kelley *et al.*, 1999). $^{240+239}\text{Pu}$ atmospheric fluxes, derived from the sediment inventories, found here are extremely large for the Southern Hemisphere, 4.9 , 1.0 , 0.5 , 2.7 , 2.0 and $3.7 \text{ mBq cm}^{-2} \text{ yr}^{-1}$ in sediment cores PA2, PA9, PA10, PP, PZC and RM respectively. Furthermore, the $^{240+239}\text{Pu}$ fluxes in this work are substantially higher than in coastal sediment cores taken on the southeastern region of Brazil ($0.10 \text{ mBq cm}^{-2} \text{ yr}^{-1}$) (Sanders *et al.*, 2010) or continental shelf (0.20 to $0.43 \text{ mBq cm}^{-2} \text{ yr}^{-1}$) (Sanders *et al.*, 2014a) of South America, supporting the assertion of high fluxes of the particle reactive Pu tracers in specific depositional settings of the Amazon Basin. The expected global fallout atmospheric flux of Pu to the sediments is $0.58 \text{ mBq cm}^{-2} \text{ yr}^{-1}$.

The $^{240+239}\text{Pu}$ inventories in this work are substantially greater than the global fallout atmospheric fluxes and greater than most other lakes around the globe. For instance, Lake Bosten, China $0.46 \text{ mBq cm}^{-2} \text{ yr}^{-1}$ (Liao *et al.*, 2014) and in Lithuania Lake $1.0 \text{ mBq cm}^{-2} \text{ yr}^{-1}$ and 0.05 to $0.32 \text{ mBq cm}^{-2} \text{ yr}^{-1}$. However the fluxes in this work are lower than what was found in NW Greenland 5.14 – $31.6 \text{ mBq cm}^{-2} \text{ yr}^{-1}$ (Lukšiene *et al.*, 2014; Mietelski *et al.*, 2016b). One of the reasons for the high fluxes found in this work is likely because $^{240+239}\text{Pu}$ deposited on land may also enter water bodies due to soil erosion and run-off processes, which then accumulate in

wetland or lake environments. For instance, forest canopies are very efficient in the initial capturing of atmospheric fallout (Iurian *et al.*, 2015; Todorović *et al.*, 2013). Therefore the inventory of anthropogenic radionuclides in sediments reflects the source function and the transport of radionuclides (Pourcelot *et al.*, 2003; Todorović *et al.*, 2013). Indeed, the highest atmospheric $^{240+239}\text{Pu}$ fluxes (PA2), derived from the inventories on Table 2, is an area open to the river floodplain lake, an indication of intense lateral transport of the particle reactive Pu.

The $^{240+239}\text{Pu}$ and ^{210}Pb methods are interpreted as having comparable sediment accretion rates in three sites (PA2, PZC, RM) and substantially different in the other three floodplain lakes (PA9, PA10, PP) (Table 2). The difference in sediment accretion rates between these two dating methods may be attributed to the different time spans these two models represent. For instance, accretion derived from $^{240+239}\text{Pu}$ represent a net accumulation rate relative to a 60-year timeframe whereas net accumulation rates calculated using the CIC approach with ^{210}Pb represents an over 100 year timescale. When comparing net accumulation rates from these two methodologies, we are assuming a consistent deposition regime across these timescales. However this may not be the case along the Amazon Basin as a result of changes in seasonal rain (El Nino) and land use activities (such as deforestation) which will influence the sediment loads that are delivered to the floodplain lakes.

The $^{210}\text{Pb}_{\text{ex}}$ inventories, shown in Table 2, give an integrated view of the sedimentary dynamics as the $^{210}\text{Pb}_{\text{ex}}$ inventories vary greatly from one floodplain lake to another. These differences in $^{210}\text{Pb}_{\text{ex}}$ inventories indicate differing depositional fluxes (Smoak *et al.*, 1996). The $^{210}\text{Pb}_{\text{ex}}$ flux to the sediments is a function of the total supply from the atmosphere, in situ production, and from creeks and rivers, all of which should be included when considering the sources of the $^{210}\text{Pb}_{\text{ex}}$ to the sedimentation inventories (Smoak *et al.*, 1996). The relatively large fluxes of $^{210}\text{Pb}_{\text{ex}}$ greatly exceeds what was measured directly from the atmospheric fallout rates ($15.3 \text{ mBq cm}^{-2} \text{ yr}^{-1}$) in South-eastern Brazil (Sanders *et al.*, 2011). Hence, the depositional inventory at the sediment coring locations in this work is far greater than the inventory of the directly deposited atmospheric flux in South-eastern Brazil. These high inventories are also noted from the $^{240+239}\text{Pu}$ profiles. This is because the initial atmospheric fallout of $^{240+239}\text{Pu}$ is fairly well known and lower than what was found in this study (Kelley *et al.*, 1999). Indeed, $^{240+239}\text{Pu}$ fluxes found here are extremely large for the Southern Hemisphere, which are reported to range from 0.20 to $0.43 \text{ mBq cm}^{-2} \text{ yr}^{-1}$ (Kelley *et al.*, 1999; Sanders *et al.*, 2010). Because the $^{240+239}\text{Pu}$ fluxes follow the same high inventories as $^{210}\text{Pb}_{\text{ex}}$, the sedimentary profiles in this work support the assertion that sediment focussing is contributing to the relatively high fluxes of the particle reactive tracers in the depositional settings of the Amazon floodplains.

5. CONCLUSION

The $^{240+239}\text{Pu}$ and ^{210}Pb sediment dates in this work indicate that the Amazon floodplain lakes accumulate sediment at rates between 2.4 and 18.6 mm year⁻¹ during the previous century. However the derived $^{240+239}\text{Pu}$ and ^{210}Pb sedimentation models produced substantially different sediment accretion rates in three of the six sites. These differences are attributed to the different time spans these independent models represent and/or the solubility of Pb and Pu along the sediment column. From the two independent dating methods used in this work which are based on different time scales, we conclude sedimentation rates have remained relatively stable near the Madera River and the $^{240+239}\text{Pu}$ and ^{210}Pb inventories indicate that there is greater sediment focusing at the Madeiras River floodplain lakes, as compared to the Tapajos and Amazon River floodplain lakes, during the previous century. Furthermore, this work shows that the detection of a recognizable $^{240+239}\text{Pu}$ in sediment profiles of the Amazon floodplain lakes is promising in terms of future uses as a geochronometric tool in the this region. The geochronologies derived from the $^{240+239}\text{Pu}$ and ^{210}Pb dating methods outlined in this work are of an ideal timeframe for studying the effects of anthropogenic influences along the Amazon Basin during the 20th century.

ACKNOWLEDGEMENTS

LMS is supported by an APA and IPRS scholarships. CJS was supported by the Australian Research Council (DE160100443, DP150103286, and LE140100083). AEP is supported by CNPq, FAPERJ and CAPES. We would like to thank Professor Donny Smoak and Professor Michael Ketterer for assisting in the sediment dating.

REFERENCES

- Abril JM, 2003. Constraints on the use of ^{137}Cs as a time-marker to support CRS and SIT chronologies. *Environmental Pollution* 129: 31–37, DOI 10.1016/j.envpol.2003.10.004.
- Alhajji E, Ismail IM, Al-Masri MS, Salman N, Al-Haleem MA and Doubal AW, 2014. Sedimentation rates in the lake Qattinah using ^{210}Pb and ^{137}Cs as geochronometer. *Geochronometria* 41: 81–86, DOI 10.2478/s13386-013-0142-5.
- Appleby PG and Oldfield F, 1992. Application of lead-210 to sedimentation studies, p. 731–783. In M. Ivanovich and S. Harmon [eds.], *Uranium Series Disequilibrium: Application to Earth, Marine and Environmental Science*. Oxford Science Publications.
- Barlow J, Lennox GD, Ferreira J, Berenguer E, Lees AC, Nally RM, Thomson JR, Ferraz SFDB, Louzada J, Oliveira VHF, Parry L, Ribeiro De Castro Solar R, Vieira ICG, Aragaõ LEOC, Begotti RA, Braga RF, Cardoso TM, Souza RCDO Jr CM, Moura NG, Nunes SS, Siqueira JV, Pardini R, Silveira JM, Vaz-De-Mello FZ, Veiga RCS, Venturieri A and Gardner TA, 2016. Anthropogenic disturbance in tropical forests can double biodiversity loss from deforestation. *Nature* 535: 144–147, DOI 10.1038/nature18326.
- Blais JM and J Kalf, 1995. The influence of lake morphometry on sediment focusing. *Limnology and Oceanography* 40: 582–588.
- Cao L, Ishii N, Zheng J, Kagami M, Pan S, Tagami K, and Uchida S, 2017. Vertical distributions of Pu and radiocesium isotopes in sediments from Lake Inba after the Fukushima Daiichi Nuclear Power Plant accident: Source identification and accumulation. *Applied Geochemistry* 78: 287–294, DOI 10.1016/j.apgeochem.2017.01.012.
- Everett SE, Tims SG, Hancock GJ, Bartley R and Fifield LK, 2008. Comparison of Pu and ^{137}Cs as tracers of soil and sediment transport in a terrestrial environment. *Journal of Environmental Radioactivity* 99: 383–393, DOI 10.1016/j.jenvrad.2007.10.019.
- Iurian AR, Dercon G, Adu-Gyamfi J, Mabit L, Kis-Benedek G, Ceccatelli A, Tarjan S and Blake W, 2015. The interception and wash-off fraction of ^7Be by bean plants in the context of its use as a soil radiotracer. *Journal of Radioanalytical and Nuclear Chemistry* 306: 301–308, DOI 10.1007/s10967-015-3948-1.
- Junk WJ, Wittmann F, Schöngart J and Piedade MTF, 2015. A classification of the major habitats of Amazonian black-water river floodplains and a comparison with their white-water counterparts. *Wetlands Ecology and Management* 23: 677–693, DOI 10.1007/s11273-015-9412-8.
- Kelley JM, Bond LA and Beasley TM, 1999. Global distribution of Pu isotopes and ^{237}Np . *Science of the Total Environment* 237–238: 483–500.
- Ketterer ME, Hafer KM, Jones VJ and Appleby PG, 2004a. Rapid dating of recent sediments in Loch Ness: Inductively coupled plasma mass spectrometric measurements of global fallout plutonium. *Science of the Total Environment* 322: 221–229, DOI 10.1016/j.scitotenv.2003.09.016.
- Ketterer ME, Hafer KM and Mieltski JW, 2004b. Resolving Chernobyl vs. global fallout contributions in soils from Poland using Plutonium atom ratios measured by inductively coupled plasma mass spectrometry. *Journal of Environmental Radioactivity* 73: 183–201, DOI 10.1016/j.jenvrad.2003.09.001.
- Ketterer ME and Szechenyi SC, 2008. Determination of plutonium and other transuranic elements by inductively coupled plasma mass spectrometry: A historical perspective and new frontiers in the environmental sciences. *Spectrochimica Acta - Part B Atomic Spectroscopy* 63: 719–737, DOI 10.1016/j.sab.2008.04.018.
- Leslie C and Hancock GJ, 2008. Estimating the date corresponding to the horizon of the first detection of ^{137}Cs and $^{239+240}\text{Pu}$ in sediment cores. *Journal of Environmental Radioactivity* 99: 483–490, DOI 10.1016/j.jenvrad.2007.08.016.
- Liao H, Bu W, Zheng J, Wu F and Yamada M, 2014. Vertical distributions of radionuclides ($^{239+240}\text{Pu}$, ^{240}Pu , and ^{137}Cs) in sediment cores of lake bosten in Northwestern China. *Environmental Science and Technology* 48: 3840–3846, DOI 10.1021/es405364m.
- Lokas E, Zwoliński Z, Rachlewicz G, Gąsiorek M, Wilkosz G and Samolej K, 2017. Distribution of anthropogenic and naturally occurring radionuclides in soils and lakes of Central Spitsbergen (Arctic). *Journal of Radioanalytical and Nuclear Chemistry* 311: 707–717, DOI 10.1007/s10967-016-5085-x.
- Lukšienė B, Maceika E, Tarasiuk N, Koviagina E, Filistovič V, Buivydas Š and Puzas A, 2014. On peculiarities of vertical distribution of $^{239,240}\text{Pu}$, ^{238}Pu and ^{137}Cs activity concentrations and their ratios in lake sediments and soils. *Journal of Radioanalytical and Nuclear Chemistry* 300: 277–286, DOI 10.1007/s10967-014-3026-0.
- Mieltski JW, Kierepko R, Lokas E, Cwanek A, Kleszcz K, Tomankiewicz E, Mróz T, Anczkiewicz R, Szalkowski M, Wąs B, Bartyzel M and Misiak R, 2016a. Combined, sequential procedure for determination of ^{137}Cs , ^{40}K , ^{63}Ni , ^{90}Sr , $^{230,232}\text{Th}$, $^{234,238}\text{U}$, ^{237}Np , $^{238,239+240}\text{Pu}$ and ^{241}Am applied for study on contamination of soils near Żarnowiec Lake (northern Poland). *Journal of Radioanalytical and Nuclear Chemistry* 310: 661–670, DOI 10.1007/s10967-016-4835-0.
- Mieltski JW, Kierepko R, Lokas E, Cwanek A, Kleszcz K, Tomankiewicz E, Mróz T, Anczkiewicz R, Szalkowski M, Wąs B, Bartyzel M and Misiak R, 2016b. Combined, sequential procedure for determination of ^{137}Cs , ^{40}K , ^{63}Ni , ^{90}Sr , $^{230,232}\text{Th}$, $^{234,238}\text{U}$, ^{237}Np , $^{238,239+240}\text{Pu}$ and ^{241}Am applied for study on contamination of soils near Żarnowiec Lake (northern Poland). *Journal of Radioanalytical and Nuclear Chemistry* 310: 661–670, DOI 10.1007/s10967-016-4835-0.

- Omokheyeke O, Sikoki FD, Laissaoui A, Akpuluma D, Onyagbodor PO, Benkdad A and Benmansour M, 2014. Sediment geochronology and spatio-temporal and vertical distributions of radionuclides in the Upper Bonny Estuary (South Nigeria). *Geochronometria* 41: 369–376, DOI 10.2478/s13386-013-0164-z.
- Pourcelot L, Louvat D, Gauthier-Lafaye F and Stille P, 2003. Formation of radioactivity enriched soils in mountain areas. *Journal of Environmental Radioactivity* 68: 215–233, DOI 10.1016/S0265-931X(03)00051-1.
- Quinto F, Hrncsek E, Krachler M, Shotyk W, Steier P and Winkler SR, 2013. Determination of ^{239}Pu , ^{240}Pu , ^{241}Pu and ^{242}Pu at femtogram and attogram levels—evidence for the migration of fallout plutonium in an ombrotrophic peat bog profile. *Environmental Sciences: Processes and Impacts* 15: 839–847, DOI 10.1039/c3em30910j.
- Rowland L, Da Costa ACL, Galbraith DR, Oliveira RS, Binks OJ, Oliveira AAR, Pullen AM, Doughty CE, Metcalfe DB, Vasconcelos SS, Ferreira LV, Malhi Y, Grace J, Mencuccini M and Meir P, 2015. Death from drought in tropical forests is triggered by hydraulics not carbon starvation. *Nature* 528: 119–122, DOI 10.1038/nature15539.
- Sanders CJ, Caldeira PP, Smoak JM, Ketterer ME, Belem A, Mendoza UMN, Cordeiro LGMS, Silva-Filho EV, Patchineelam SR and Albuquerque ALS, 2014a. Recent organic carbon accumulation (~100 years) along the Cabo Frio, Brazil upwelling region. *Continental Shelf Research* 75: 68–75, DOI 10.1016/j.csr.2013.10.009.
- Sanders CJ, Eyre BD, Santos IR, MacHado W, Luiz-Silva W, Smoak JM, Breithaupt JL, Ketterer ME, Sanders L, Marotta H and Silva-Filho E, 2014b. Elevated rates of organic carbon, nitrogen, and phosphorus accumulation in a highly impacted mangrove wetland. *Geophysical Research Letters* 41: 2475–2480, DOI 10.1002/2014GL059789.
- Sanders CJ, Santos IR, Maher DT, Breithaupt JL, Smoak JM, Ketterer M, Call M, Sanders L and Eyre BD, 2016. Examining $^{239+240}\text{Pu}$, ^{210}Pb and historical events to determine carbon, nitrogen and phosphorus burial in mangrove sediments of Moreton Bay, Australia. *Journal of Environmental Radioactivity* 151: 623–629, DOI 10.1016/j.jenvrad.2015.04.018.
- Sanders CJ, Smoak JM, Cable PH, Patchineelam SR and Sanders LM, 2011. Lead-210 and Beryllium-7 fallout rates on the southeastern coast of Brazil. *Journal of Environmental Radioactivity* 102: 1122–1125, DOI 10.1016/j.jenvrad.2011.07.008.
- Sanders CJ, Smoak JM, Sanders LM, Waters MN, Patchineelam SR and Ketterer ME, 2010. Intertidal mangrove mudflat $^{240+239}\text{Pu}$ signatures, confirming a ^{210}Pb geochronology on the southeastern coast of Brazil. *Journal of Radioanalytical and Nuclear Chemistry* 283: 593–596, DOI 10.1007/s10967-009-0418-7.
- Smoak JM, Demaster DJ, Kuehl SA, Pope RH and McKee BA, 1996. The behavior of particle-reactive tracers in a high turbidity environment: ^{234}Th and ^{210}Pb on the Amazon continental shelf. *Geochimica et Cosmochimica Acta* 60: 2123–2137, DOI 10.1016/0016-7037(96)00092-0.
- Tims SG, Tsifakis D, Srnčik M, Keith Fifield L, Hancock GJ and De Cesare M, 2013. Measurements of low-level anthropogenic radionuclides from soils around Maralinga. EPJ Web of Conferences, DOI 10.1051/epjconf/20136303010.
- Todorović D, Popović D, Ajtić J and Nikolić J, 2013. Leaves of higher plants as biomonitors of radionuclides (^{137}Cs , ^{40}K , ^{210}Pb and ^7Be) in urban air. *Environmental Science and Pollution Research* 20: 525–532, DOI 10.1007/s11356-012-0940-y.
- Wu F, Zheng J, Liao H, Yamada M and Wan G, 2011. Anomalous plutonium isotopic ratios in sediments of lake Qinghai from the Qinghai-Tibetan Plateau, China. *Environmental Science and Technology* 45: 9188–9194, DOI 10.1021/es202315c.
- Zheng J, Tagami K, Watanabe Y, Uchida S, Aono T, Ishii N, Yoshida S, Kubota Y, Fuma S and Ihara S, 2012. Isotopic evidence of plutonium release into the environment from the Fukushima DNPP accident. *Scientific Reports* 2, DOI 10.1038/srep00304.
- Zheng J and Yamada M, 2004. Sediment core record of global fallout and bikini close-in fallout Pu in Sagami Bay, Western Northwest Pacific margin. *Environmental Science and Technology* 38: 3498–3504, DOI 10.1021/es0351931.